18

Development of a Yeast Two-Hybrid Screen for Selection of Human Ras–Raf Protein Interaction Inhibitors

Vladimir Khazak, Erica A. Golemis, and Lutz Weber

Summary

A yeast two-hybrid screening system was developed to screen for small molecules that inhibit the interaction of the Ras and the Raf proteins. Hyperpermeable yeast strains useful for high-throughput screening (HTS) for the two-hybrid system were created. Differential inhibition of the Ras–Raf vs the hsRPB4–hsRPB7 interaction allowed the identification of selective inhibitors.

Key Words: Ras; Raf; yeast two-hybrid system; protein interaction; compound library; cell-based screening.

1. Introduction

With recent advances in genome-wide sequencing, studies of the function of individual proteins and protein complexes have become increasingly important for understanding biological functions, and for selection of novel targets for drug discovery applications. The yeast two-hybrid system was originally developed to identify and study protein–protein interactions *(1,2)*. This method was later expanded to allow detection of interactions between proteins and RNA *(3)*, proteins and nonprotein ligands *(4)*, proteins and peptides *(5)*, proteins and multiple partners *(6,7)*, and whole-genome applications *(8–10)*. In addition, some investigators have begun to study the potential of two-hybrid screens to detect protein–small-molecule interactions *(11–13)*. However, limited progress has so far been made to adapt such yeast screening technologies for the identification of new clinical candidates in high-throughput screens (HTSs).

One major barrier to the use of yeast for drug screening has been thought to be the relative impermeability of yeast cells to a broad spectrum of organic molecules.

From: *Methods in Molecular Biology, vol. 310: Chemical Genomics: Reviews and Protocols*
Edited by: E. D. Zanders © Humana Press Inc., Totowa, NJ

Physical and chemical genetic techniques have been used to enhance the permeability of yeast membranes. Permeabilizing agents, such as polymyxin B sulfate and polymyxin B nonapeptide, have been used to physically disrupt the integrity of yeast membranes (**14**). However, use of such chemical agents in drug screening is not ideal, because of the toxicity induced by polymyxin B treatment.

As an alternative strategy, a number of yeast genes involved in the control of membrane permeability have been identified, which might be targeted to improve strain permeability (**15**). In particular, a network of regulators associated with the phenotype known as pleiotropic drug resistance (PDR), which closely resembles the mammalian multi-drug resistance phenotype (MDR) (**16**), is known to affect cellular transport and drug resistance. Pdrlp and Pdr3p, members of the C6 zinc cluster family of transcriptional regulatory proteins, redundantly modulate expression of ABC transporter proteins by inducing their transcription (**17**,**18**). Disruption of *PDRI* and *PDR3*, the genes encoding Pdrlp and Pdr3p, respectively, results in decreased expression of the ABC transporter *PDR5*, and thereby increases drug sensitivity of *pdr1*$^{-}$*pdr3*$^{-}$ cells (**19**). Further, it has been shown that overexpression of either the HXT9p or HXT11p hexose transporter proteins independently promotes drug sensitivity, by increasing uptake of certain drugs (**19**,**20**). Based on these earlier studies, we have exploited these properties of PDR and HXT mutants to create hyperpermeable yeast strains useful for HTS for the two-hybrid system. We here describe the creation of these strains and their utilization for the selection of small-molecule inhibitors of interaction between Ras and Raf oncoproteins.

2. Materials

1. Yeast *Saccharomyces cerevisiae* strains SKY48 (*MAT*α *trp1 URA3 his3 6 lexAop-LEU2 cIop- LYS2*) and SKY191 (*MAT*α *trp1 URA3 his3 2 lexAop-LEU2 cIop-LYS2*) have been described in (**1**).
2. *Escherichia coli* strain DH5α.
3. pGem-T/A (Promega, Madison, WI).
4. DBD and AD plasmids for yeast two-hybrid screen have been described in (**1**,**21**).
5. Restriction enzymes T4 DNA ligase and Taq DNA polymerase (MBI Fermentas).
6. Oligonucleotide primers.
7. Yeast dropout (DO) media, YPD (rich medium with dextrose), and YPG/R (rich medium with galactose and raffinose) (Clontech, CA).
8. Cycloheximide (CYH), 4-nitroquinoline-oxide (4-NQO), sulfomethuron methyl (SMM), and 5-fluoro-orotic acid (5FOA) (BioMol, PA).
9. Zeocin (Zeo) (Invitrogen, CA).
10. X-Gal (Clontech, CA).
11. 96-pin replicator (Nalge Nunc International Corp., IL).

3. Methods

The methods outlined below describe (1) the construction of expression plasmids bearing conditionally regulated yeast *HXT9* and *HXT11* hexose transporter genes, (2) integration of *HXT9*- and *HXT11*-containing DNA fragments in the *PDR1* and *PDR3* chromosomal loci of yeast two-hybrid strains, (3) analysis of the permeability of newly developed yeast strains with selected known small-molecule inhibitors, and by screen of a large combinatorial library of compounds, and (4) selection of inhibitors of the interaction between human Ras and Raf-1 by screening the combinatorial library of compounds in the obtained hyperpermeable yeast two-hybrid strain.

3.1. Expression Plasmids

In order to enhance the permeability of the yeast *S. cerevisiae* to small-molecular-weight compounds, the two yeast hexose transporters *HXT9* and *HXT11* were subcloned under control of the galactose-inducible *GAL1* promoter and subsequently integrated by homologous recombination into the genetic loci for *PDR1* and *PDR3*, thereby destroying the coding sequence of these genes. The cloning and integration strategies are presented in flow charts (**Figs. 1** and **2**). Additional maps for cloning intermediates are available upon request. All polymerase chain reaction (PCR) primer sequences are shown in **Table 1**.

3.1.1. Construction of the pPDR1-HisCadA Plasmid

Primers VK11 and VK14 were used to amplify an 1158-base-pair (bp) 5' fragment of *PDR1*, and primers VK12 and VK13 were used to amplify a 741-bp 3' fragment of *PDR1*, using PCR. The amplified *PDR1* fragments were cloned into pGem-T/A (Promega, Madison, WI) to construct the pGem5-3-*PDR1* plasmid, with a unique BamHI site between the fragments. Next, the pHisCadA plasmid was constructed by replacing the *Salmonella hisG* DNA fragment in the pNKY51 plasmid with the *E. coli cadBA* gene operon. Next, the *hisG-URA3-cadA* gene fragment from pHis-*CadA* was isolated, purified, and ligated into the BamHI site of the pGem5-3-*PDR1* vector to construct the pPDR1-His*CadA* plasmid (**Fig. 3A**) (*see* **Note 1**).

3.1.2. Construction of the pPDR3-HisInt Plasmid

Primers VK07 and VKl0 were used to amplify an 839-bp 5' fragment of the yeast *PDR3* gene, and VK09 and VK11 were used to amplify a 743-bp 3' fragment of the yeast *PDR3* gene. The amplified fragments were then cloned into pGem-T/A to create pGEM5-3-PDR3, which bears a unique BamHI site between the *PDR3* fragments. The pHisInt plasmid was then constructed by replacing the *hisG* 3' fragment of the pNKY51 plasmid with a fragment from the human

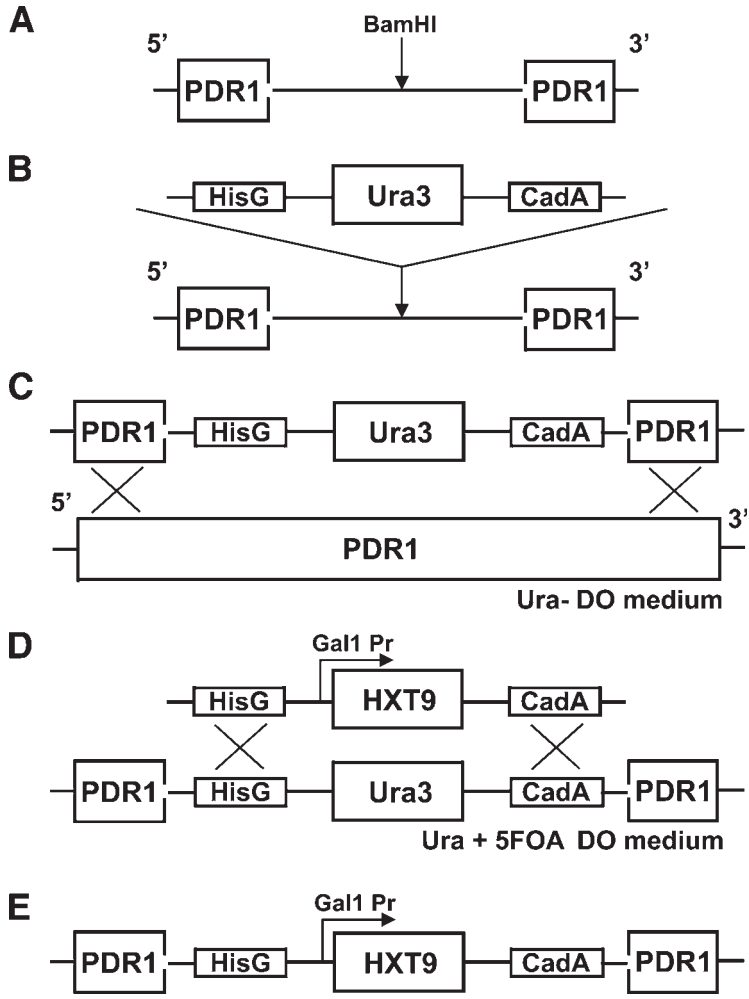

Fig. 1. In the first step of the integrative transformation strategy used to construct the modified yeast strains SKY51 and SKY194: the *HXT9* gene is targeted to the yeast *PDR1* locus. **(A)** A plasmid vector containing upstream (5') and downstream (3') flanking regions of the *PDR1* gene separated by a unique restriction site (BamHI). **(B)** An integrative cassette containing *hisG-URA3-cadA* is inserted at the unique BamHI site between the *PDR1* gene fragments. **(C)** The structure of the recombination intermediate containing a *PDR1* gene disrupted by the *hisG-URA3-cadA* cassette is shown. **(D)** Recombination between *hisG* and *cadA* sequences of the *hisG-URA3-cadA* cassette on the chromosome and the *hisG* and *cadA* sequences on separately prepared linear *hisG-HXT9-cadA* cassette is detected by growth on 5FOA (i.e., *ura3-* phenotype), which reflects insertion of *HXT9* into the chromosomal location of the *PDR1* gene with loss of PDR1 and URA3. **(E)** The genomic structure of the *PDR1* locus of the modified yeast strains SKY51 and SKY194, derived from SKY48 and SKY191, respectively.

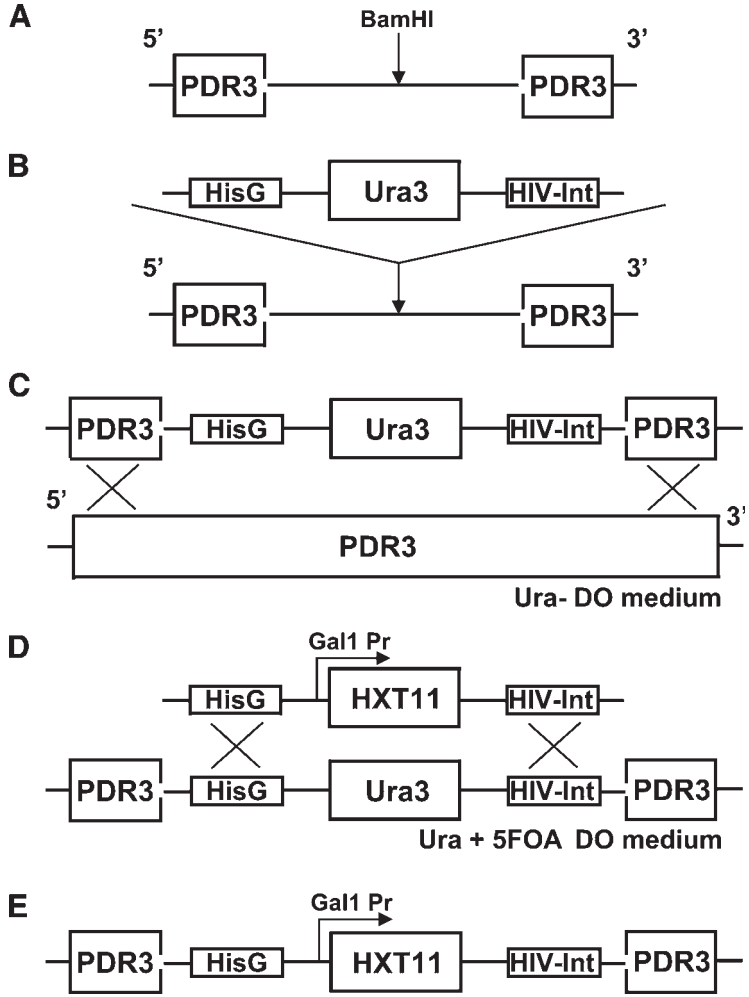

Fig. 2. In a second step of the integrative transformation strategy used to construct the modified yeast strains SKY54 and SKY197 from strains SKY51 and SKY194, the *HXT11* gene is targeted to the yeast *PDR3* locus. **(A)** Plasmid vector was constructed containing the upstream (5') and downstream (3') flanking regions of the *PDR3* gene separated by a unique restriction site (BamHI). **(B)** An integrative cassette containing *hisG-URA3-Int* was inserted at the unique BamHI site between the *PDR3* gene fragments. This was used for integration by homologous replacement of *PDR3* as selected by a *ura*-phenotype. **(C)** The structure of recombination intermediate containing a *PDR3* gene disrupted by the *hisG-URA3-Int* cassette is shown. **(D)** Next, homologous recombination between *hisG* and *Int* sequences of the integrated *hisG-URA3-Int* cassette on the chromosome and a separately prepared, linear *hisG-HXT11-Int* cassette results in insertion of the *HXT11* gene at the endogenous yeast *PDR3*1ocus as selected by growth on 5FOA media. **(E)** The genomic structure of the *PDR3* locus of the final yeast strains, SKY54 and SKY197.

Table 1
Oligonucleotide Primers Used in Plasmid and Strain Construction

Primer	Sequence (5' +-3')	Description
VK03	CTCAAGCTTATGTCAGGTGTTAATAATACATCC	Forward HXT11
VK04	CCGAAAACTTCTAGATCAGCTGGAAAAG	Reverse HXT11
VK05	CTTACCCAAGCTTATGTCCGGTGTTAAT	Forward HXT9
VK06	ACCTCTAGATTAGCTGGAAAAGAACCTC	Reverse HXT9
VK07	TTAATTTTTTCTTATTGCGTGACCG	Forward PDR3
VK08	TGGTTATGCTCTGCTTCCCTATTTC	Reverse PDR3
VK09	AAAGGATCCTTTTATGTGGAAGACCCGCA	Forward PDR3 from 2188bp
VK10	TTTGGATCCATTAACATCGATGAACCCGTGT	Reverse PDR3 from 839bp
VK11	CAGAAAAGAATCCAAGAAACGGAAG	Forward PDR1
VK12	GAGAACTTTTATCTATACAAACGTATACG	Reverse PDR1
VK13	TTTGGATCCTGACAATCGTCACTCG	Forward PDR1 from 2466bp
VK14	TTAGGATCCTCACAAAGGGCTGCGGTA	Reverse PDR1 from 1158bp
VK15	GGAAGAATTATTTCTGGCCTAGG	Forward HXT9 and HXT11 from 505bp
VK16	AATAGACACGTACGGCGTCC	Reverse HXT9 and HXT11 from 1161bp
VK22	AAAGAAGCTAATCTGTAAACGCAGGTC	Reverse cadA from 3667bp of HisHXT9cadA cassette
VK23	GGAAGAGGTTATCGCCCTGC	Forward hisG from 829bp of HisHXT11INT cassette
VK24	CCCTGCACTGTACCCCCC	Reverse HIVInt from 4093p of HisHXT11INT cassette

immunodeficiency virus (HIV) integrase gene (*Int*) (*see* **Note 1**). The *hisG-URA3-Int* fragment was then isolated, purified, and ligated into the BamHI site of the pGem5-3-PDR3 vector to create the pPDR3-HisInt plasmid (**Fig. 3B**).

3.1.3. Construction of the pHisCadA-HXT9 Plasmid

Primers VK05 and VK06 were used to PCR amplify the coding sequence of the yeast *HXT9* gene. The *HXT9* gene fragment was ligated downstream of the *GAL1*-inducible promoter and upstream of the *CYC1* transcription terminator region (TT) in the pYES2 plasmid to create the pYES-HXT9 plasmid. The fragment containing the *GAL1* promoter region, the *HXT9* gene fragment, and the *CYC1* TT region from pYES-HXT9 were then ligated into pHisCadA (see above) to create pHisCadA-HXT9 (**Fig. 3C**) (*see* **Note 2**).

3.1.4. Construction of the pHisInt-HXT11 Plasmid

Primers VK03 and VK04 were used to PCR amplify the coding sequence of the yeast *HXT11* gene. The *HXT11* fragment was ligated downstream of the *GAL1*-inducible promoter and upstream of the *CYC1* TT region in the pYES2 plasmid to create the pYES-HXT11 plasmid. The fragment containing the *GAL1* promoter region, the *HXT11* coding region, and the *CYC1* TT region from pYes-HXT11 were then excised, purified, and ligated into pHisInt to create pHisInt-HXT11 (**Fig. 3D**).

3.2. Integration of HXT9 and HXT11 in the PDR1 and PDR3 Chromosomal Loci of Yeast S. cerevisiae *Strains SKY48 and SKY191*

In order to integrate conditionally expressed *HXT9* and *HXT11* transporter genes in a yeast two-hybrid genetic background ***(1)***, the expression plasmids from **Subheading 3.1.** were digested with restriction enzymes, and DNA fragments containing the target genes were purified and used for subsequent site-specific chromosomal recombination (*see* **Figs. 1** and **2**). Yeast transformed with these plasmids were selected based on a URA3+ phenotype, and subsequently characterized by PCR of genomic DNA to confirm that correct integrations had occurred.

3.2.1. Constructing Yeast S. cerevisiae *Strains SKY49 and SKY192*

The plasmid pPDR3-HisInt was digested with AatII-SacI and the purified integrative cassette, *hisG-URA3-PDR3-Int* (*see* **Fig. 2C**) was transformed into parental strains SKY48 and SKY191. Positive cells were selected on yeast drop-out media that lacked uracil. Cells that grew on such media contained integrated copies of *hisG-URA3-Int* cassette and were designated SKY49 and SKY192.

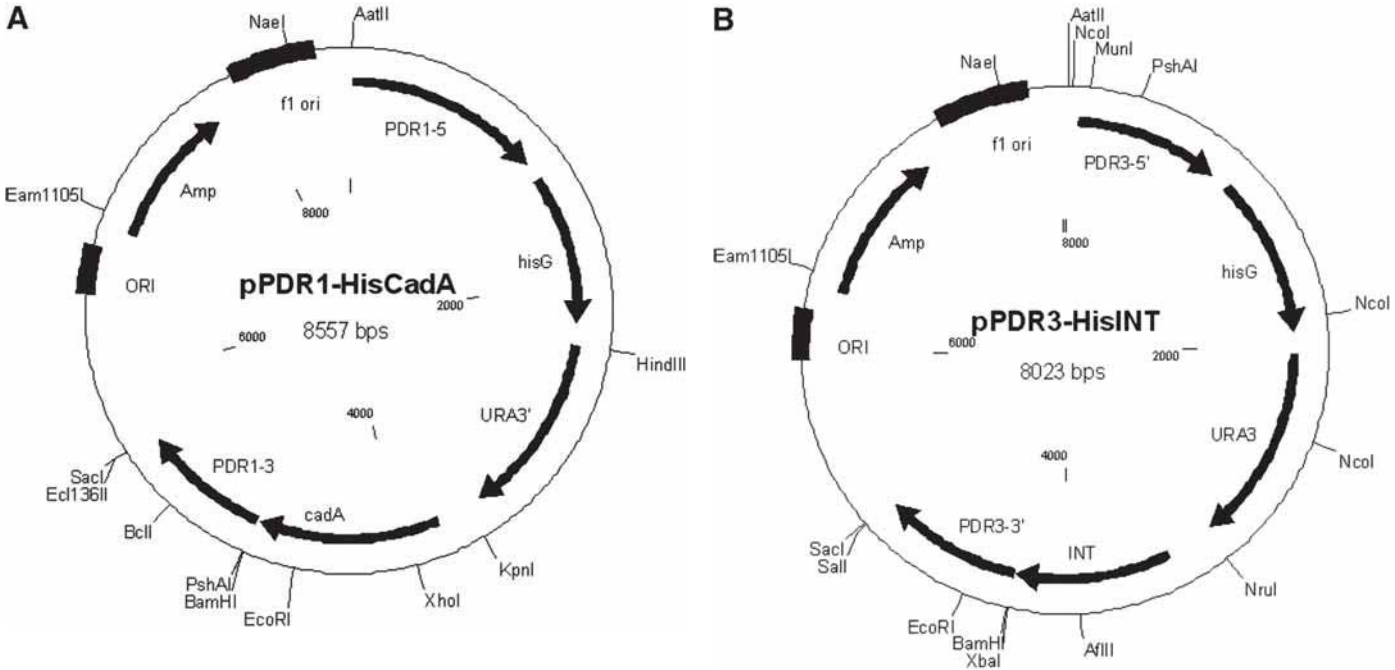

Fig. 3. Plasmid maps. **(A)** Map of the pPDRI-HisCadA plasmid. The *hisG-URA3-cadA* gene fragment is flanked by upstream (PDR1-5') and downstream (PDRl-3') sequences of *PDR1*, as indicated. This is the source of the *PDR1-hisG-URA3-cadA-PDR1* cassette (**Fig. 1**). **(B)** Map of the pPDR3-HisInt plasmid. The *hisG-URA3-Int* gene fragment is flanked by upstream (PDR3-5') and downstream (PDR3-3') sequences of *PDR3*, as indicated. This is the source of the *PDR3-hisG-URA3-Int-PDR3* cassette (**Fig. 2**).

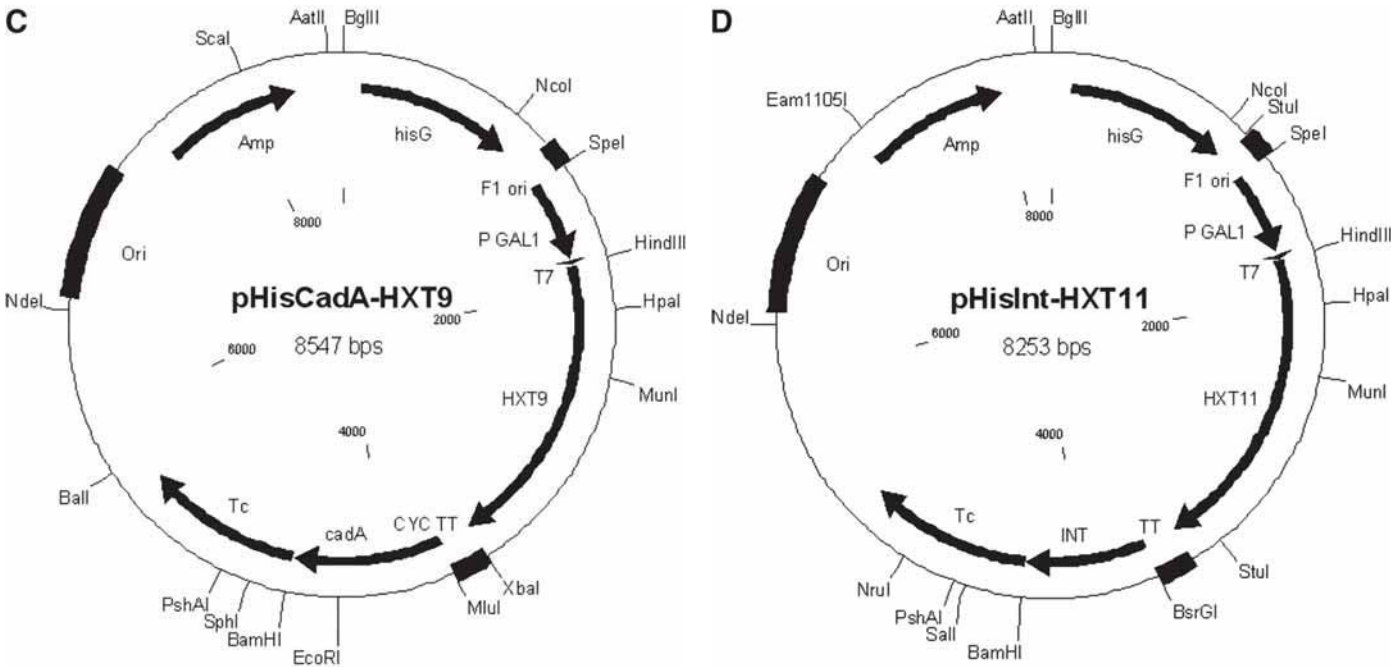

Fig. 3. **(C)** Map of the pHisCadA-HXT9 plasmid. The P GAL1- HXT9 -CYC1-TT is inserted upstream from *Escherichia coli cadBA* gene operon (cadA). This is the source of the *hisG-HXT9-cadA* cassette (**Fig. 1**). **(D)** Map of the pHisInt-HXT11 plasmid. The P GALl- HXT11-CYC1-TT is inserted upstream from human immunodeficiency virus (HIV) integrase gene sequences (INT). This is the source of the *hisG-HXT11-Int* cassette (**Fig. 2**).

3.2.2. Constructing Yeast S. cerevisiae Strains SKY51 and SKY194 With Galactose-Inducible HXT11 Gene Integrated in PDR3 Chromosomal Locus

Strains SKY49 and SKY192 were used for the next round of integrative transformation. The goal of this transformation was to replace the *URA3* gene at the *PDR3* locus in the chromosome of SKY49 and SKY192 with a galactose-inducible copy of *HXT11*. To this end, plasmid pHisHXT11-Int was digested with AatII and PshAI, and the *hisG-HXT11-Int* cassette was purified and transformed into SKY49 and SKY192. To select yeast with the *hisG-HXT11-Int* cassette integrated into the chromosome, cells were propagated on YPD plates for 5–6 h to decrease the amount of Ura3p enzyme, and then replica-plated on plates containing minimal DO media containing 1.5 mg/mL 5-fluoro-orotic acid (5FOA) and uracil at a concentration of 1.2 mg/mL (*see* **Note 3**). Yeast that express the *URA3* gene convert 5FOA to a toxic metabolite and die. However, cells that have replaced the *URA3* gene with *HXT11* grow normally. Several hundred transformants containing the *HXT11* gene at the *PDR3* chromosomal locus were obtained. Two strains containing the inserted cassettes (**Fig. 2C**) were selected, and named SKY51 and SKY194.

3.2.3. Constructing Yeast S. cerevisiae Strains SKY54 and SKY197 Bearing Galactose-Inducible HXT9 and HXT11 Genes in PDR1 and PDR3 Loci

At the next round of integrative transformation, the *hisG-URA3-cadA* cassette in pPDR1-HisCadA was digested with AatII-SacI and the purified cassette (**Fig. 1C**) was transformed into SKY51 and SKY194. Two resulting yeast strains, SKY52 and SKY195, were selected on yeast dropout media that lacked uracil. The *hisG-HXT9-cadA* cassette was then purified and transformed into SKY52 and SKY195, thereby replacing the *hisG-URA3-cadA* cassette with the *hisG-HXT9-cadA* cassette. Another round of 5FOA selection (*see* **Fig. 1D**) yielded two strains, SKY54 and SKY197, with *HXT9* substituted for *URA3* at the *PDR1* locus (*see* **Fig. 1E**).

Cells selected after this final round of integrative transformation have integrated copies of *HXT9* and *HXT11* at the *PDR1* and *PDR3* loci, respectively. The full genotype of SKY54 is *(MATα trp1 ura3 his3 3lexAop-Leu2 1cIop-Lys2 pdr1::HXT9 pdr3::HXT11)*, and that of SKY197 is *(MATα trp1 ura3 his31lexAop-Leu2 1cIop-Lys2 pdr1::HXT9 pdr3::HXT11)*.

3.2.4. Characterization of SKY54 and SKY197

To confirm the proper insertion of *HXT9* and *HXT11* into the chromosomal loci of *PDR3* and *PDR1*, respectively, genomic DNA was purified from SKY54 and SKY197, and analyzed using PCR for the presence of *HXT9* and *HXT11*

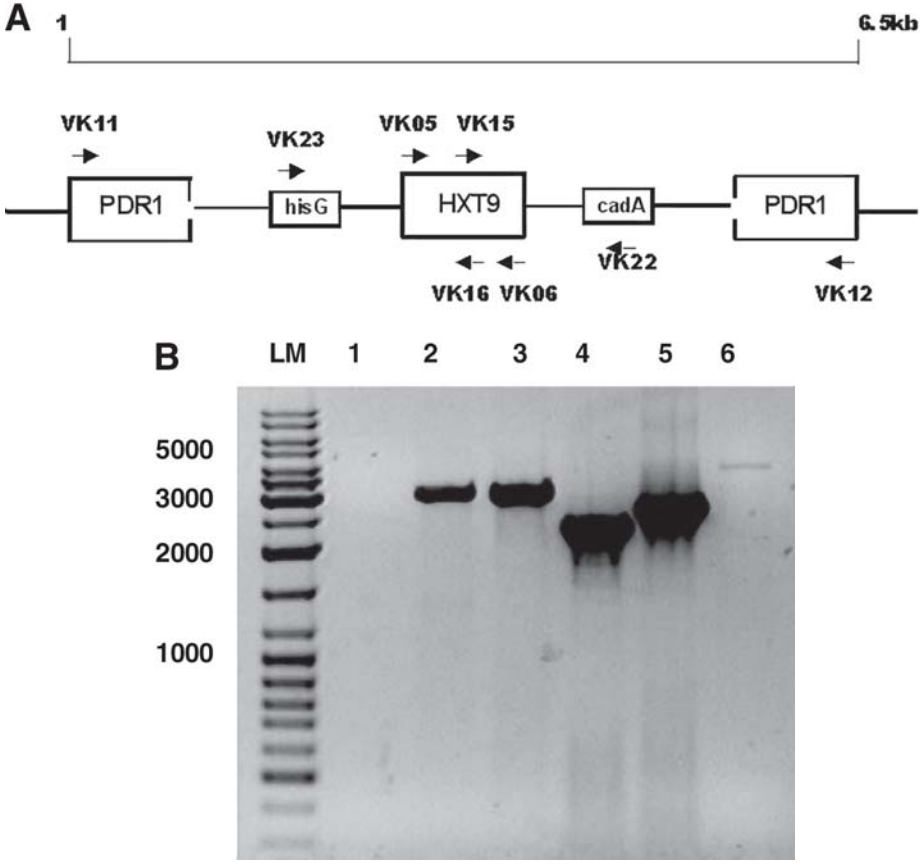

Fig. 4. Structure of the inserted *HXT9* gene sequence at the yeast *PDR1* locus in strains SKY54 and SKY197. **(A)** is a diagram of the structure of the inserted DNA sequence at the *PDR1* locus. **(B)** is an ethidium bromide-stained gel of polymerase chain reaction products, confirming the integration of recombinant *HXT9* sequences at the *PDR1* locus: LM—Ladder Mix DNA standard (MBI Fermentas); 1—VK11–VK22 (SKY197); 2—VK15–VK12 (SKY197); 3—VK15–VK12 (SKY54); 4—VK15–VK22 (SKY54); 5—VK23–VK06 (SKY54); 6—VK23–VK22 (SKY54).

recombinant sequences within *PDR1 and PDR3* loci. (**Figs. 4A,B** and **5A,B**). **Figure 4A** depicts the DNA fragment *PDR1-hisG-HXT9-cadA-PDR1*, which was inserted into the *PDR1* locus of SKY54 and SKY197, showing the location and orientation of PCR primers. **Figure 4B** shows an agarose gel stained with ethidium bromide to visualize the PCR products. The six bands correspond to the proper lengths between the specific primer pairs, and confirm the correct

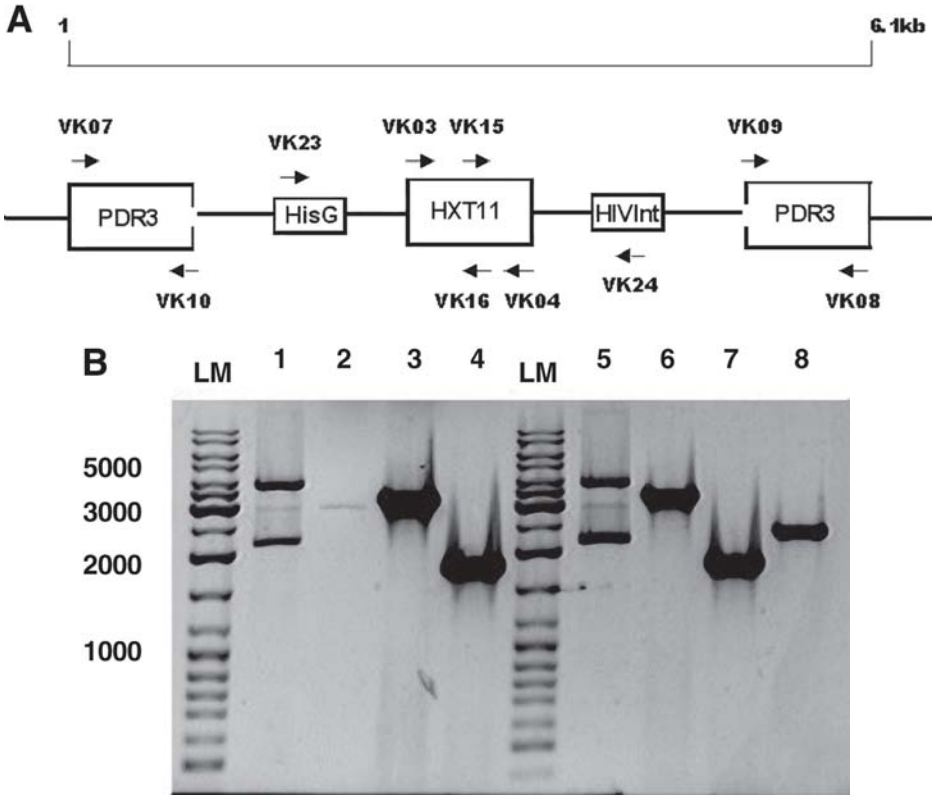

Fig. 5. Structure of the inserted *HXT11* DNA sequence at the yeast *PDR3* locus in strains SKY54 and SKY197. **(A)** is a diagram of the structure of the inserted DNA sequence at the *PDR3* locus. **(B)** is an ethidium bromide-stained agarose gel of polymerase chain reaction products, confirming the integration of recombinant *HXT11* sequences at the *PDR3* locus: LM—Ladder Mix DNA standard (MBI Fermentas); 1—VK07–VK16 (SKY197) (top band); 2—VK15–VK08 (SKY197); 3—VK23–VK24 (SKY197); 4—VK15–VK24 (SKY197); 5—VK07–VK16 (SKY54) (top band); 6—VK23–VK24 (SKY54); 7—VK15–VK24 (SKY54); 8—VK03–VK24 (SKY197).

insertion and orientation of the cassettes. **Figure 5A** depicts the DNA fragment *PDR3-hisG-HXT11-Int-PDR3* that was inserted into the *PDR3* locus of SKY54 and SKY197, indicating the location and direction of PCR primers. **Fig. 5B** shows an ethidium bromide-stained gel of the PCR products. The eight bands correspond to the proper lengths between the specific primer pairs indicated, and confirm the correct insertion and orientation of the cassettes.

3.3. Testing the Permeability (Sensitivity) of Yeast Strains SKY54 and SKY197 With Targeted Antifungals, and to a Diverse Chemical Library of Small-Molecular-Weight Compounds

To test the new strains for enhanced permeability to small-molecular-weight inhibitors, SKY54 and SKY197 and their parental strains were incubated with various concentrations of selected antifungal compounds, and with a diverse combinatorial library of uncharacterized compounds.

3.3.1. SKY54 and SKY197 Have Increased Sensitivity to Selected Antifungal Inhibitors

Cycloheximide (CYH), 4-nitroquinoline-oxide (4-NQO), sulfomethuron methyl (SMM) and Zeocin (Zeo) were used to evaluate the drug sensitivity of the yeast strains. Yeast cells were seeded as a lawn on YPD or YPG/R plates by being dispersed in a "pad" of top agar poured over a normal plate (100 µL of resuspended yeast [10^8 cells] to 13 mL of cooled 1% low-melt SeaPlaque agarose prepared with YPD or YPG/R growth media). Immediately after seeding, CYH (5 mg/mL), NQO (2.5 mg/mL), SMM (100 mg/mL), and Zeo (100 mg/mL) stock solutions were diluted 2-, 5-, 10-, 25-, and 100-fold, and applied onto the top-agar growing yeast by means of a pronged replicator device that delivered 1-µL liquid aliquots of compound into the top-agar layer. Sensitivity to compounds was scored by visualization of growth on this media, and the size of "death zones" around areas of compound application.

The plates shown in **Fig. 6** demonstrate the sensitivity of the parental and modified yeast strains to the test compounds. Both parental SKY191 and modified SKY197 strains showed no sensitivity to SMM at all concentrations tested. However, based on the size of the death zones, SKY197 is significantly more sensitive to CYH and 4-NQO than SKY191 on YPD media (**Fig. 6**). Further, when the SKY197 yeast were incubated on Gal/Raff-containing media (thereby inducing expression of *HXT9* and *HXT11* genes), their sensitivity to CYH and 4-NQO increased. The estimated increase of death-zone diameters for 4-NQO for SKY197 on YPG/R media in comparison with the parental strains grown on the same media was approx 32–40%. After 48 h of incubation on YPG/R media, sensitivity to CYH was estimated to be 0.01 µg/mL minimal inhibitory concentration (MIC) in comparison to 0.5 µg/mL for the parental strain. The MIC is defined as the lowest concentration (micrograms per milliliter of broth) that inhibited visible growth, disregarding a haze of barely visible growth. Sensitivity to CYH of a yeast strain harboring *PDR1* and *PDR3* deletions, and with the *HXT11* gene overexpressed from a multicopy plasmid, was previously reported as having an MIC of 0.03 µg/mL CYH ***(19)***. Thus, integrating inducible copies of *HXT11* and *HXT9* into the chromosome while deleting *pdr1* and *pdr3*

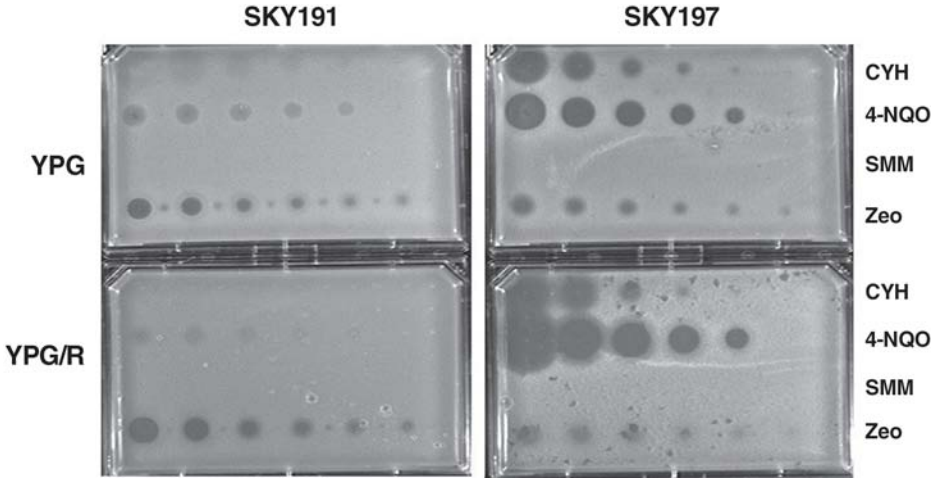

Fig. 6. Sensitivity of the modified yeast strain SKY197, relative to the unmodified parental strain SKY191, to various compounds. Decreasing concentrations of cycloheximide (CYH), 4-nitroquinoline-oxide (4-NQO), sulfomethuron methyl (SMM), and Zeocin (Zeo) were plated on parental yeast strain SKY191 and the modified strain SKY197, and incubated on YPD (Glu) or YPG/R (Gal/Raff) media. From top to bottom of each plate, and from left to right of each row: 5 µg, 2.5 µg, 1 µg, 0.5 µg, 0.2 µg, and 50 ng of CYH; 2.5 µg, 1.25 µg, 0.5 µg, 0.25 µg, 0.1 µg, and 25 ng of NQO; 100 µg, 50 µg, 20 µg, 10 µg, 4 µg, and 1 µg of SMM; and 100 µg, 50 µg, 20 µg, 10 µg, 4 µg, and 1 µg of Zeo.

significantly increased the sensitivity of yeast cells to the tested compounds (*see* **Note 4**).

3.3.2. SKY54 Has Increased Sensitivity to a Diverse Chemical Library of Small-Molecular-Weight Compounds

A comparative analysis of parental strain SKY48 and its derivative SKY54 to 73,400 compounds from the diverse combinatorial chemical library is shown in **Table 2**. SKY48 was sensitive to 1959 compounds, while SKY54 was sensitive to 3011 compounds. Thus, SKY54 was sensitive to 1.54 times as many compounds as the parental strain, SKY48. The sensitivity/permeability of modified yeast SKY54 and SKY197 was similar to the permeability of *E. coli* strains specifically designed for HTS purposes, and screened with the same library of compounds (data not shown). This fact created a unique opportunity to use modified yeast two-hybrid strains SKY54 and SKY197 for screening of various protein–protein interaction inhibitors.

Table 2
Sensitivity of Yeast SKY48 and SKY54 to a Library of Small-Molecule Compounds

Strain	No. Compounds Tested	No. of Hits	% of Hits
SKY 48	73,400	1959	2.7
SKY54	73,400	3011	4.1

3.4. Selecting Novel Inhibitors of Ras-Raf Interaction by High-Throughput Screening in SKY54 Dual-Bait Yeast Two-Hybrid Strain

The Ras/Raf/MEK/ERK signaling pathway controls fundamental cellular processes including proliferation, differentiation, and survival, and the altered expression or action of components of this pathway is commonly observed in human cancers *(22–24)*. Ras has suffered oncogenic mutations in nearly 30% of human cancers and mediates its action through interaction with downstream effector targets *(25,26)*. Activated Ras binds to and recruits Raf-1 to the cell membrane, where Raf-1 is activated by a complex mechanism that is not yet completely understood *(27)*. Agents capable of inhibiting the activating interaction between oncogenic Ras and Raf proteins have the potential to be valuable additions to the chemotherapy of multiple cancers. The human Ras and Raf proteins effectively interact in a yeast two-hybrid system *(28)*, which makes this interaction an attractive drug target in yeast strains with increased permeability.

To screen for chemical compounds that would effectively block or diminish the interaction between a DNA binding domain (DBD) fusion to Ras (cI-H-Ras) and an activation domain (AD) fused Raf (AD-c-Raf-1), while simultaneously testing the properties of the new permeable yeast strains, these two fusion proteins were expressed in SKY54, and in parallel in SKY48, and plated as described under **Subheading 3.3.1.**, with the addition of X-Gal. Yeast containing an independent interacting protein pair, DBD-fused-hsRPB7 and AD-hsRPB4, were similarly plated in parallel in both strains, as a control to be used for detection and subtraction of toxic compounds. These strains were used to screen a library of 73,400 compounds applied in microarray format. A representative panel demonstrating specific vs nonspecific inhibition of growth is shown in **Fig. 7**. From 3009 compounds that produced growth-inhibiting effects in the SKY54 CI-H-Ras-AD-Raf-1 strain, 708 compounds also reduced β-galactosidase activity, with varying degrees of selectivity for Ras-Raf-1 vs hsRPB7-hsRPB4 on plates. Significantly fewer positive colonies were detected in the screen performed for Ras-Raf interaction inhibitors in the SKY48 yeast strain (data not shown). Further assessment of the selectivity of interaction inhibition by liquid

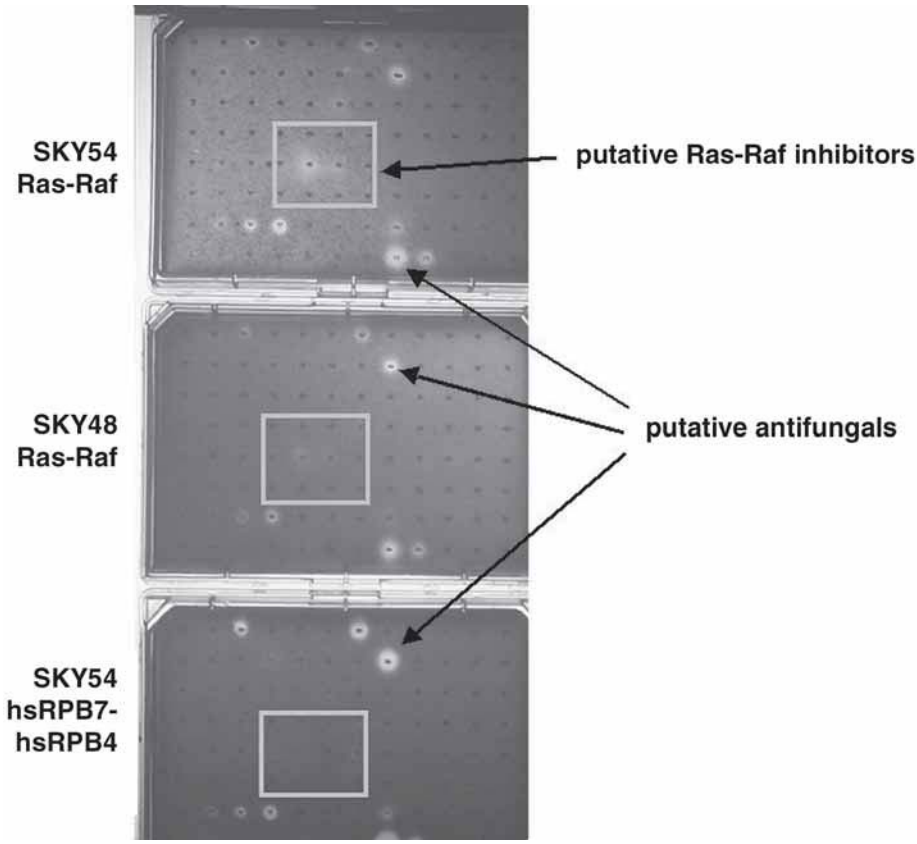

Fig. 7. Screening plates with yeast SKY54 Ras-Raf, SKY54 hsRPB4-hsRPB7, and SKY48 Ras-Raf strains incubated with the 96 compounds from combinatorial chemical library. The area with putative Ras-Raf inhibitors and individual antifungal compounds is indicated by frame or by arrow, respectively. Note increased size of "death zones" for some compounds on SKY54 vs SKY48 plates.

beta-galactosidase assay *(29)* identified 38 compounds that produced a clear reduction (with a final range of 3–45% of starting values) in *LacZ* activity in SKY54 expressing H-Ras and Raf-1, but not LexA-hsRPB7 and AD-hsRPB4, when included in culture medium at concentrations of 30 μ*M*. These 38 compounds, reflecting a yield of approx 0.05% from the starting library, were used for subsequent functional analyses in mammalian cells, that have extensively validated their mechanism of action, as described in *(30)*.

Here, we have reported a general approach for creating a super-permeable yeast two-hybrid strain, and the application of this strain for HTS for identifi-

cation of novel protein–protein interaction inhibitors. The developed strains were successfully used for screening a diverse combinatorial library to select a novel class of clinically relevant protein-protein interaction inhibitors, and have the potential to be used in future efforts to search for new drugs in two-hybrid HTS.

4. Notes

1. Our choice of the *hisG* DNA fragment from *Salmonella*, *cadBA* gene from *E. coli*, and the *Int* gene from the *HIV* virus was based on the lack of sequences homologous to these DNA sequences in yeast. Thus, the chromosomal integration of the expression cassettes was directed to the specific sites intended (*PDR1*, *PDR3*) through homologous recombination. The specific DNAs we have used can be successfully replaced in integration cassettes by other DNA sequences that have no or low homology to yeast genomic DNA.
2. *GAL1* was chosen as a promoter because of its strength and inducible nature. Further, comparison of the yeast sensitivity to the given compound on media supplemented with glucose (YPD) vs galactose (YPG) allows unequivocal estimation of the contribution of the *HXT9* gene to the reduction of resistance phenotype.
3. We found that the Ura3p enzyme synthesized from the first integration cassette is present in the yeast cells at the time of addition of 5FOA compound even in the cells with a successful second cassette integration and elimination of an active copy of *URA3* gene. The activity of these remnants of Ura3p causes the conversion of 5FOA into a toxic metabolite, and subsequent cell death. Additional propagation of the yeast on the YPD media, rich in exogenous uracil, is sufficient to significantly reduce the level of the earlier synthesized Ura3p enzyme in the cells with successful recombinations, and escape from 5FOA-related toxicity.
4. The absence of improved sensitivity to SMM and Zeo in the modified SKY197 strain indicates that the enhancement of permeability is not universal, but limited to some compound classes, likely reflecting differences in the uptake and efflux mechanisms for different drugs.

Acknowledgments

The authors thank Dr. Antonios Makris for providing the cDNA encoding the human H-Ras and Raf-1 genes. We also thank Dr. Alan Hinnebusch for providing the pNKY51 plasmid. EG was supported by NIH core grant CA-06927, and an appropriation from the Commonwealth of Pennsylvania (to Fox Chase Cancer Center).

References

1. Serebriiskii, I., Khazak, V., and Golemis, E. A. (1999) A two-hybrid dual bait system to discriminate specificity of protein interactions. *J. Biol. Chem.* **274,** 17,080–17,087.
2. Fields, S. and Song, O. (1989) A novel genetic system to detect protein-protein interactions. *Nature* **340,** 245–246.

3. SenGupta, D. J., Zhang, B., Kraemer, B., Pochart, P., Fields, S., and Wickens, M. (1996) A three-hybrid system to detect RNA-protein interactions in vivo. *Proc. Natl. Acad. Sci. USA* **93,** 8496–8501.
4. Meyerson, M., Enders, G. H., Wu, C. L., et al. (1992) A family of human cdc2-related protein kinases. *EMBO J.* **11,** 2909–2917.
5. Colas, P., Cohen, B., Jessen, T., Grishina, I., McCoy, J., and Brent, R. (1996) Genetic selection of peptide aptamers that recognize and inhibit cyclin-dependent kinase 2. *Nature* **380,** 548–550.
6. Osborne, M. A., Zenner, G., Lubinus, M., et al. (1996) The inositol 5'-phosphatase SHIP binds to immunoreceptor signaling motifs and responds to high affinity IgE receptor aggregation. *J. Biol. Chem.* **271,** 29,271–29,278.
7. Tirode, F., Malaguti, C., Romero, F., Attar, R., Camonis, J., and Egly, J. M. (1997) A conditionally expressed third partner stabilizes or prevents the formation of a transcriptional activator in a three-hybrid system. *J. Biol. Chem.* **272,** 22,995–22,999.
8. Fromont-Racine, M., Rain, J. C., and Legrain, P. (1997) Toward a functional analysis of the yeast genome through exhaustive two-hybrid screens. *Nat. Genet.* **16,** 277–282.
9. Finley, R. L. Jr. and Brent, R. (1994) Interaction mating reveals binary and ternary connections between *Drosophila* cell cycle regulators. *Proc. Natl. Acad. Sci. USA* **91,** 12,980–12,984.
10. Bartel, P. L., Roecklein, J. A., SenGupta, D., and Fields, S. (1996) A protein linkage map of Escherichia coli bacteriophage T7. *Nat. Genet.* **12,** 72–77.
11. Young, K., Lin, S., Sun, L., et al. (1998) Identification of a calcium channel modulator using a high throughput yeast two-hybrid screen. *Nat. Biotechnol.* **16,** 946–950.
12. Vidal, M., Brachmann, R. K., Fattaey, A., Harlow, E., and Boeke, J. D. (1996) Reverse two-hybrid and one-hybrid systems to detect dissociation of protein-protein and DNA-protein interactions. *Proc. Natl. Acad. Sci. USA* **93,** 10,315–10,320.
13. Liu, G., Thomas, L., Warren, R. A., et al. (1997) Cytoskeletal protein ABP-280 directs the intracellular trafficking of furin and modulates proprotein processing in the endocytic pathway. *J. Cell Biol.* **139,** 1719–1733.
14. Boguslawski, G. (1985) Effects of polymyxin B sulfate and polymyxin B nonapeptide on growth and permeability of the yeast *Saccharomyces cerevisiae*. *Mol. Gen. Genet.* **199,** 401–405.
15. Brendel, M. (1976) A simple method for the isolation and characterization of thymidylate uptaking mutants in *Saccharomyces cerevisiae*. *Mol. Gen. Genet.* **147,** 209–215.
16. Marger, M. D. and Saier, M. H. Jr. (1993) A major superfamily of transmembrane facilitators that catalyse uniport, symport and antiport. *Trends Biochem. Sci.* **18,** 13–20.
17. Katzmann, D. J., Burnett, P. E., Golin, J., Mahe, Y., and Moye-Rowley, W. S. (1994) Transcriptional control of the yeast PDR5 gene by the PDR3 gene product. *Mol. Cell Biol.* **14,** 4653–4661.

18. Saunders, G. W. and Rank, G. H. (1982) Allelism of pleiotropic drug resistance in *Saccharomyces cerevisiae*. *Can. J. Genet. Cytol.* **24,** 493–503.
19. Nourani, A., Wesolowski-Louvel, M., Delaveau, T., Jacq, C., and Delahodde, A. (1997) Multiple-drug-resistance phenomenon in the yeast *Saccharomyces cerevisiae*: involvement of two hexose transporters. *Mol. Cell Biol.* **17,** 5453–5460.
20. Kruckeberg, A. L. (1996) The hexose transporter family of *Saccharomyces cerevisiae*. *Arch. Microbiol.* **166,** 283–292.
21. Khazak, V., Estojak, J., Cho, H., et al. (1998) Analysis of the interaction of the novel RNA polymerase II (pol II) subunit hsRPB4 with its partner hsRPB7 and with pol II. *Mol. Cell Biol.* **18,** 1935–1945.
22. Panaretto, B. A. (1994) Aspects of growth factor signal transduction in the cell cytoplasm. *J. Cell Sci.* **107(Pt 4),** 747–752.
23. Pawson, T. (1993) Signal transduction—a conserved pathway from the membrane to the nucleus. *Dev. Genet.* **14,** 333–338.
24. Egan, S. E. and Weinberg, R. A. (1993) The pathway to signal achievement. *Nature* **365,** 781–783.
25. Marshall, C. J. (1996) Ras effectors. *Curr. Opin. Cell Biol.* **8,** 197–204.
26. Khosravi-Far, R., Campbell, S., Rossman, K. L., and Der, C. J. (1998) Increasing complexity of Ras signal transduction: involvement of Rho family proteins. *Adv. Cancer Res.* **72,** 57–107.
27. Kolch, W. (2000) Meaningful relationships: the regulation of the Ras/Raf/MEK/ERK pathway by protein interactions. *Biochem. J.* **351(Pt 2),** 289–305.
28. Vojtek, A. B., Hollenberg, S. M., and Cooper, J. A. (1993) Mammalian Ras interacts directly with the serine/threonine kinase Raf. *Cell* **74,** 205–214.
29. Ausubel, F. M., Brent, R., Kingston, R., et al. (1994-present) *Current Protocols in Molecular Biology*, John Wiley & Sons, New York.
30. Kato-Stankiewicz, J., Hakimi, I., Zhi, G., et al. (2002) Inhibitors of Ras/Raf-1 interaction identified by two-hybrid screening revert Ras-dependent transformation phenotypes in human cancer cells. *Proc. Natl. Acad. Sci. USA* **99,** 14,398–14,403.